5B.1 CAN'T SEE THE FOREST FOR THE TREES: METHODS FOR THE ANALYSIS AND VISUALIZATION OF LARGE RADAR DATASETS

John D. Tuttle and Richard E. Carbone*

National Center for Atmospheric Research†, Boulder, Colorado.

1. INTRODUCTION

In the case study approach of a precipitation event two dimensional images (PPIs, RHIs, etc.) of radar data are often examined frame by frame (as a function of time) in order to understand the evolution and dynamics of the event. When dealing with several weeks, months or even years of data, however, such approaches often end in frustration and little understanding is gained from the massive amounts of radar images. If we are to study the precipitation cycle and understand its relationship to forcing mechanisms (synoptic, density currents, diurnal heating, etc.) for a long time series, other approaches that reduce the volume of data to a manageable level can provide more insight. One approach is to reduce the dimensions of the dataset by averaging in one spatial dimension (latitude or longitude) and plotting the data in the remaining spatial dimension as a function of time (time-longitude or time-latitude). Such plots are often referred to as Hovmoller diagrams and have been used in the climatology community for many years. In the Hovmoller diagrams coherent precipitation episodes travelling across the continent appear as streaks, and patterns associated with different types of forcing are revealed. From the streaks, statistics on the propagation speed, span (km) and duration (h) of the precipitation event are easily obtained. The averaging can also be done over time (as a function of the diurnal cycle) and data plotted in longitude-latitude space. This approach is not limited to radar data and when combined with satellite, model analysis and lightning data becomes even more powerful.

2. METHODOLOGY

The primary data used here are the WSI Corporation NOWrad TM national composite radar reflectivity. The properties of this product include ~2 km latitude/longitude grid with 15 minute temporal resolution and 16 levels of reflectivity at 5 dBZ intervals. The WSI data are resampled on a 0.2^o latitude/longitude grid where the number of data points greater than 15, 25, 35, 45, and 55 dBZ in each 0.2^o box is calculated (the average value is also found) and the statistics are written out in CEDRIC format (Mohr et al., 1986). The purpose of this step is to reduce the dataset to a manageable size allowing several years of data to fit on standard computer disk and to bring data from various sources into a common format (CEDRIC). The CEDRIC data are then read into the Hovmoller software (plot_hov) for analysis and display.

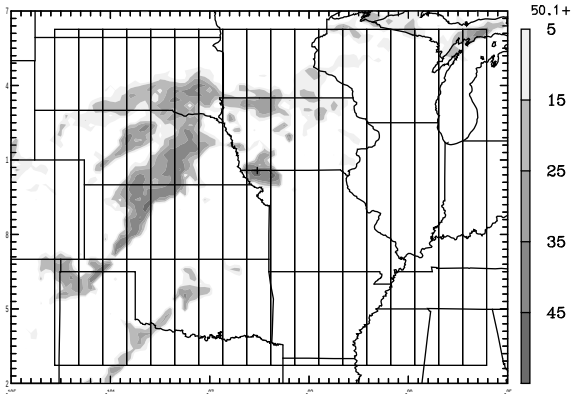

Fig. 1. Schematic showing a computational domain for a time-longitude Hovmoller plot. Data are averaged within each vertical slab. For clarity the slabs are shown much wider than the actual 0.2^o used. Background radar reflectivity is shown at 0600 UTC on 16 June 1996.

The basic procedure is shown schematically in Fig. 1 where the 0.2^o reflectivity data at a particular time are divided into a series of longitude slabs. The data are averaged in each slab in the latitudinal direction. By repeating the process for different times, a time-longitude plot can be built. Using constant latitude slabs and averaging in the longitudinal direction results in a time-latitude plot. Data can also be averaged over the diurnal cycle where data from several days are summed in 1-hour bins according to the time of collection, normalized and plotted in latitude-longitude, time-longitude or time-latitude space.

3. RESULTS

Fig. 2 shows a time-longitude diagram for a strong synoptically forced event over a seven-day period in June 1996. The data shown represent the number of 0.2^o data points that exceeded 25 dBZ in each longitude slab. The dominant feature is the broad band of reflectivity moving diagonally across the plot from about 105 W, 19960615 0000 UTC (15 July 1996) to 75 W, 19960619 1200 UTC. The average slope corresponds to a speed of ~6 m s^{-1} and represents the envelope of precipitation associated with a low pressure system that moved

* Corresponding author address: John Tuttle, NCAR, P.O. Box 3000, Boulder, CO 80307-3000. email:tuttle@ucar.edu

† The National Center for Atmospheric Research is sponsored by the National Science Foundation.

across the continental U.S. Embedded within the envelope are streaks of precipitation of shorter duration and length. They have an average propagation speed of 14 m s^{-1}, more than doubled that of the low pressure. These represent precipitation associated with individual MCSs that initiated within the envelope of favorable forcing. Developing their own internal forcing mechanisms (cold pools, gravity waves, etc.), the MCSs propagated out ahead of the favorable synoptic forcing zone and eventually dissipated. Note that the MCSs mostly initiate near the time of maximum solar heating (0000). Outside of the favorable forcing envelope convection was short-lived, non-propagating and was strongly tied to the diurnal cycle.

A time-longitude Hovmoller for 20-30 July 1998 is shown in Fig. 3. The strong diurnal forcing of convection is clearly evident over the Rocky Mountains (115-105 W) and to a lesser extent over the Appalachians (85-80 W). A more interesting aspect of Fig. 3 are the streaks of propagating convection that originated nearly every day at ~105 W and 0000 UTC. Many had phase speeds ~12-14 m s^{-1}, traveled 100s of km and lasted 24 hours or longer. Carbone et al. (2002) compiled statistics on warm season precipitation episodes over a four year period and found a high frequency of long-lived events.

Data for the month of July 1998 are accumulated in 1-hour bins over the diurnal cycle and are shown in Fig. 4. The data are normalized by the number of samples in each bin and at a given time and longitude represent the percentage of time that a longitude slab had reflectivity of greater than 25 dBZ anywhere in it. The most striking feature is the convection propagating eastward starting at 0000 and 105 W. Initially the propagation is slow (~10 m s^{-1}), but as the convection becomes organized accelerates to ~20 m s^{-1}. The result is a nocturnal maximum in convection over the central U.S. Note the minimum in convection over the central U.S. at the time of solar heating maximum (0000, 100-90 W). When considering that Fig. 4 shows a 31-day average, it is quite remarkable that the likelyhood of convection exceeds 50% in many locations.

The time accumulated data can also be displayed in longitude-latitude format and animated to show the average evolution of convection tied to the diurnal forcing.

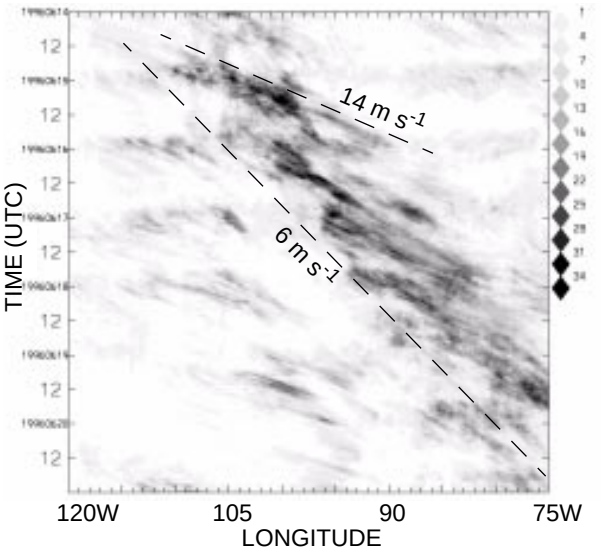

Fig. 2. Time-longitude plot of reflectivity frequency greater than 25 dBZ for 14-20 June 1996. Dashed lines show reference speeds of 6 and 14 m s^{-1} corresponding to the propagation speeds of the low pressure system and MCSs, respectively.

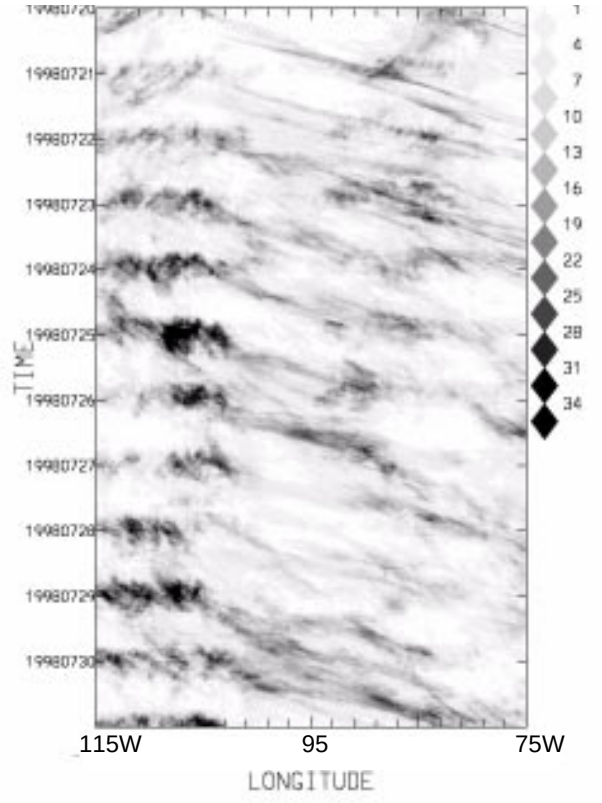

Fig. 3. Time-longitude diagram of reflectivity frequency for 20-30 July 1998.

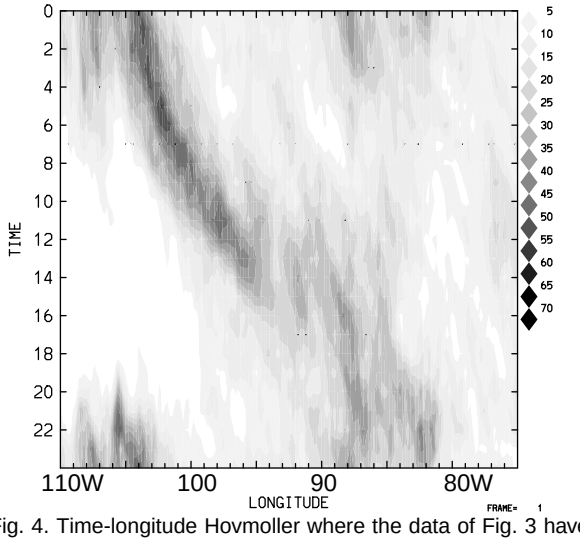

Fig. 4. Time-longitude Hovmoller where the data of Fig. 3 have been accumulated in 1-hour bins over the diurnal cycle.

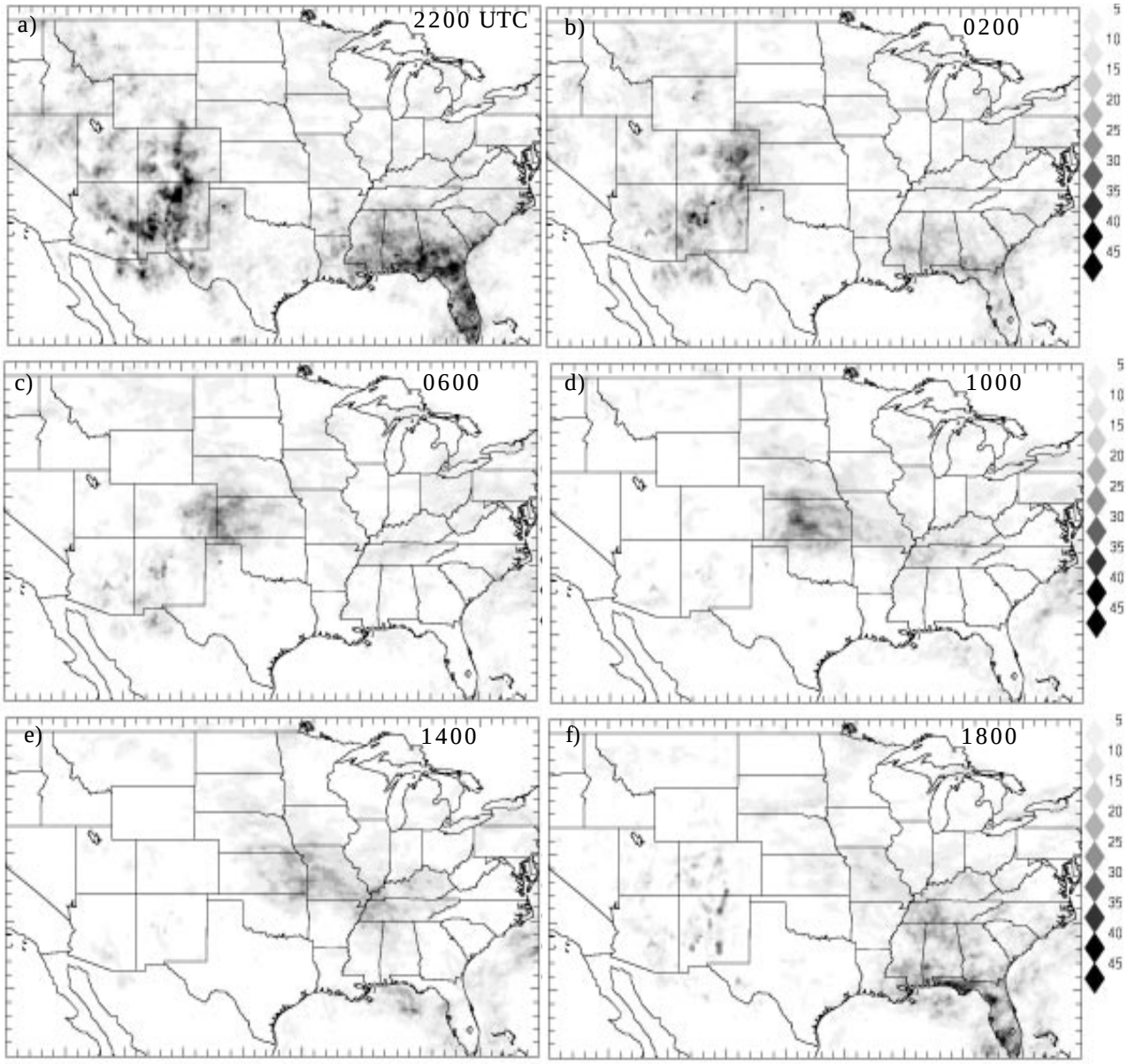

Fig. 5. Percentage of time that a location had reflectivity exceeding 25 dBZ for the month of July 1998. Data were accumulated into 1-hour bins centered on the time indicated.

Fig. 5 shows time-averaged data for the month of July 1998 at selected times. Again the data have been normalized to show the percentage of time that any location had echoes exceeding 24 dBZ. Fig. 5a is at the time of maximum solar heating. Two areas of convection are evident- one over the gulf coast/Florida peninsula and the other over the southern and central Rocky Mountain region. By 0200 (Fig. 5b) the convection in the two regions has weakened, but that over the Rockies has started to propagate eastward off the elevated terrain. During the 0600-1000 time period (fig. 5c-d), the convection that developed over Colorado moved into central Kansas producing a nocturnal maximum in convection there. Elsewhere most of the convection had dissipated. Note that convection along the Gulf coast had mostly moved offshore in response to the offshore land-sea breeze. Shortly after sunrise the convection had moved into Missouri (Fig. 5e) and eventually moved into the Tennessee valley where it merged and interacted with the Gulf coast convection (Fig 5f). Fig. 5 represents the average conditions for the entire month of July 1998. It is interesting that the convection that was able to propagate across the U.S. was confined to a relatively narrow latitudinal corridor. This same trend has been observed in other years, only the corridor shifts northward or southward. For example in July 2002, a time of record drought in the central Rockies, the main corridor of convection was shifted well to the north near the U.S.-Cana-

dian border (Fig. 6). Note the almost complete lack of propagating convection emanating from the central Rocky Mountain region (compare to Fig. 5d).

By combining radar data with model analyzed fields (CAPE, moisture, low-level shear, etc.) it is hoped that the corridors where convection is more likely to propagate long distances can be identified and forecasted. Fig. 7 shows an example of how radar and RUC (Rapid Update Cycle) fields can be combined to identify environmental variables important for sustaining convection. In this case reflectivity is overlaid on the RUC 925 hPa mixing ratio and 925-650 hPa shear vector for a two day time period. The convection initiated over southwestern Montana, travelled eastward across North Dakota and upon entering Minnesota at 1400 on July 14 encountered very moist, unstable air. The system continued moving east, but the cold-pool generated by the system interacted with the moist southerly flow to initiate a second system that moved southward and became a bow echo. The important thing to note is that the corridor of maximum mixing ratio (and maximum CAPE) is shifted ~200 km to the west of the corridor of maximum low-level shear and that the storm followed almost exactly the corridor of most favorable shear. For details of this case see Tuttle and Carbone (2003).

4. DISCUSSION

We have demonstrated the utility of analyzing and visualizing large amounts of data in reduced dimensions where data are averaged along one dimension (longitude, latitude or time) and displayed in the remaining two dimensions. Hovmoller plots allow large scale patterns to emerge that would be almost impossible to see by looking at frame after frame of two-dimensional x-y data. The plots also demonstrated that propagating convection is often confined to relatively narrow latitudinal corridors. By combining the radar data with model data it is hoped that such corridors can be identified, thereby leading to an improvement in QPF..

The source code for the software and the radar database (June-August, 1996-2002) used here may be obtained from the corresponding author.

5. REFERENCES

Carbone, R.E., J.D. Tuttle, D.A. Ahijevcy, and S.B. Trier, 2002: Inferences of predictability associated with warm season precipitation episodes. *J. Atmos. Sc*i.,**59**,2033-2056.

Mohr,C.G., L.J. Miller, R.L. Vaughan, and H.W. Frank, 1986: On the merger of mesoscale data sets into a common Cartesian format for efficient and systematic analysis. *J. Atmos. Oceanic Technol.*,**3**,143-161.

Tuttle, J.D. and R.E. Carbone, 2003: Coherent regeneration and the role of water vapor and shear in a long-lived convective episode. Submitted to *Mon. Wea. Rev.*

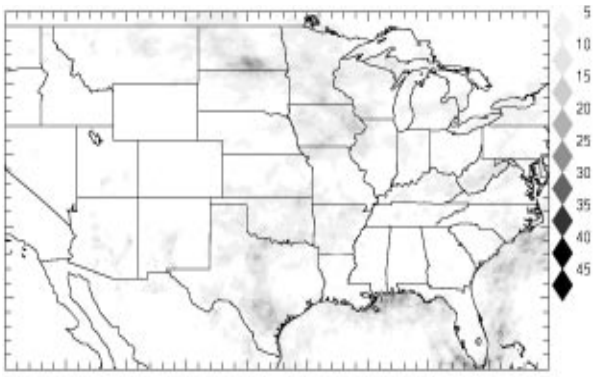

Fig. 6. Same as Fig. 5 except for July 2002 and at 1000 UTC.

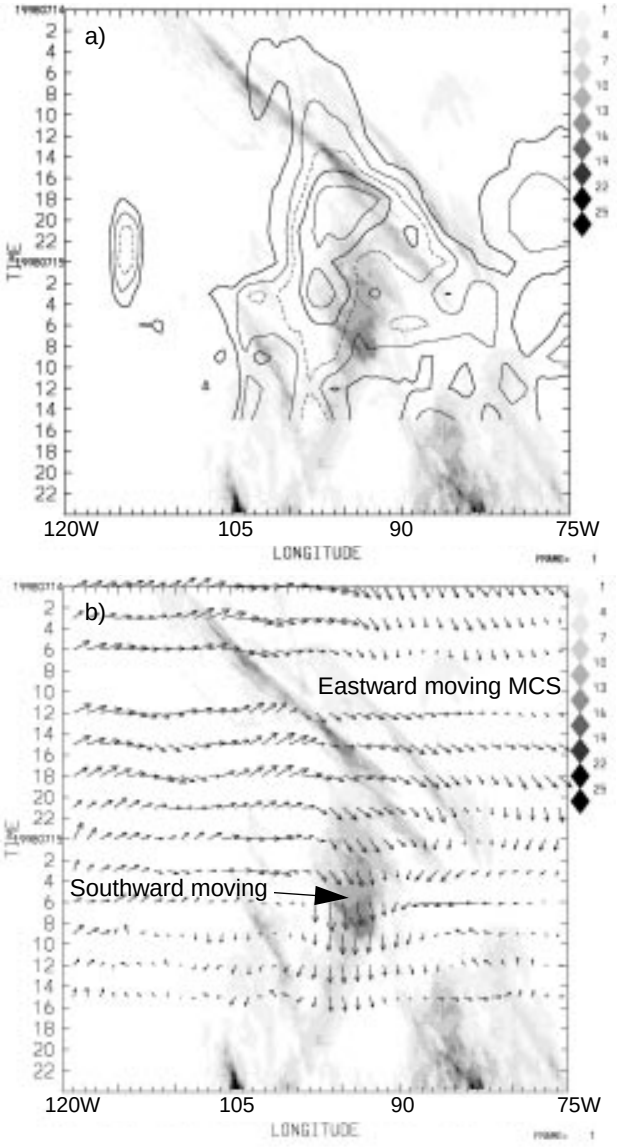

Fig. 7. Time-longitude plot of reflectivity overlaid with RUC a) 925 hPa mixing ratio and b) 925-650 hPa low-level wind shear for 14-15 July 1998. Contours of mixing ratio start at 12 g kg^{-1} and increment by 1.5. For the shear vectors north is directed toward the top of the page in the usual sense.